

Modeling and Empirical Characterization of the Polarization Response of Off-plane Reflection Gratings

HANNAH MARLOWE^{1,*}, RANDALL L. MCENTAFFER¹, JAMES H. TUTT¹, CASEY T. DEROO¹, DREW M. MILES¹, LEONID I. GORAY^{2,3,4}, VICTOR SOLTWISCH⁵, FRANK SCHOLZE⁵, ANALIA FERNANDEZ HERRERO⁵, AND CHRISTIAN LAUBIS⁵

¹The University of Iowa, 203 Van Allen Hall, Iowa City, Iowa 52242, USA

²Saint Petersburg Academic University, Khlopin 8/3 Let. A, St. Petersburg 194021, Russia

³Institute for Analytical Instrumentation, Rizhsky Prospect 26, St. Petersburg 190103, Russia

⁴ITMO University, Kronverkskiy pr. 49, St. Petersburg 197101, Russia

⁵Physikalisch-Technische Bundesanstalt (PTB), Abbestraße 2 – 12, D – 10 587 Berlin, Germany

* Hannah Marlowe: hannah-marlowe@uiowa.edu

Compiled June 19, 2016

Off-Plane reflection gratings were previously predicted to have different efficiencies when the incident light is polarized in the transverse-magnetic (TM) versus transverse-electric (TE) orientations with respect to the grating grooves. However, more recent theoretical calculations which rigorously account for finitely conducting, rather than perfectly conducting, grating materials no longer predict significant polarization sensitivity. We present the first empirical results for radially ruled, laminar groove profile gratings in the off-plane mount which demonstrate no difference in TM versus TE efficiency across our entire 300–1500 eV bandpass. These measurements together with the recent theoretical results confirm that grazing incidence off-plane reflection gratings using real, not perfectly conducting, materials are not polarization sensitive. © 2016 Optical Society of America

OCIS codes: (050.1950) Diffraction gratings; (120.2130) Ellipsometry and polarimetry; (040.7480) X-rays, soft x-rays, extreme ultraviolet (EUV); (350.1260) Astronomical optics; (340.6720) Synchrotron radiation.

<http://dx.doi.org/10.1364/ao.XX.XXXXXX>

1. INTRODUCTION

Off-plane reflection gratings offer a promising method to reach the high resolution and throughput required by the next generation of soft X-ray observatories [1, 2]. The conical diffraction pattern of the off-plane (or ‘conical’) mount lends itself to favorable packing geometries compared to gratings in the in-plane mount. Gratings may also be blazed to preferentially disperse light to a single side of zero order, thereby increasing signal to noise in those orders and reducing the required detecting area.

There have been significant discrepancies in the recent literature as to whether X-ray reflection gratings in the off-plane mount exhibit strong polarization sensitivity. Off-plane gratings were previously predicted to exhibit significant differences in efficiencies when linearly polarized light is incident in the transverse-magnetic (TM) orientation compared to transverse-electric (TE) [3]. And, indeed, a difference in efficiency between the two polarization orientations was later reported for a 14° blazed off-plane reflection grating by Seely et al. 2006 [4]. However, the measured efficiency difference did not follow the theoretical predictions. More recent theoretical calculations by Goray

& Schmidt 2010 [5] show that the predicted polarization dependence largely disappears when calculations are carried out with rigorous treatment for the finite conductivity of the grating surface as opposed to the simplifying assumption of perfect conductivity applied in the previous studies. However, no experimental measurements have so far been reported that confirm this response.

Any variation in efficiency between linear polarization orientations should be well understood to employ off-plane gratings on future missions. Without sufficient knowledge of the inherent instrumental polarization sensitivity, measurements of polarized sources could be modulated by an unknown and potentially energy dependent factor based upon observational orientation. Moreover, well characterized polarization sensitivity of off-plane gratings could offer a way to extend the polarimetry capabilities of future X-ray missions in the soft X-ray regime. To reexamine the potential polarization sensitivity of X-ray reflection gratings in the extreme off-plane mount, we performed efficiency measurements of laminar profile gratings at the Physikalisch-Technische Bundesanstalt (PTB) beamline at the BESSY II synchrotron facility between 300–1500 eV. In this paper we compare

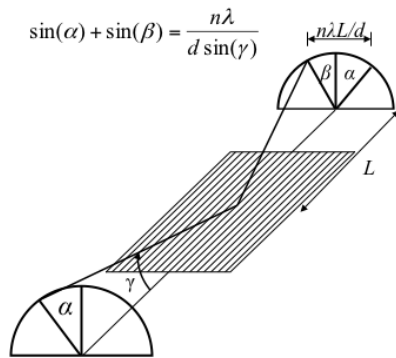


Fig. 1. Geometry of the off-plane grating mount[2].

our measurements to theoretical predictions and find good agreement with models for real, finitely conducting gratings. The experimental setup for this study is described in §2, results and modeling in §3, extension to measurements of blazed gratings in §4, and discussion is given in §5. Portions of this work were published at SPIE 9603: Optics for EUV, X-Ray, and Gamma-Ray Astronomy VII in 2015, paper number 960318 [7].

2. TEST METHODOLOGY

A. Off-plane Geometry

A diagram of the off-plane grating geometry is shown in Figure 1. In the off-plane mount, light that is incident onto the gratings at a grazing angle and quasi-parallel to the groove direction is diffracted into an arc. The diffraction equation for the off-plane mount is

$$\sin \alpha + \sin \beta = \frac{n\lambda}{d \sin \gamma}, \quad (1)$$

where γ is the polar angle of the incident X-rays defined from the groove axis at the point of intersection, d is the line spacing of the grooves, α represents the azimuthal angle along a cone with half-angle γ , and β is the azimuthal angle of the diffracted light. The grooves are radially ruled such that the spacing between adjacent grooves decreases toward the focus to match the convergence of a telescope for a spectrometer instrument. Radial ruling minimizes groove profile-induced aberration by ensuring a constant α for all rays at the grating surface and constant β per wavelength at the focal plane [2].

For gratings in the off-plane mount, we refer to linearly polarized light whose electric field vector lies in the plane defined by the incident ray and the grating normal as TE polarization (p polarization), and define TM polarization as when the electric field vector lies in the plane of the grating (s polarization). This is in contrast to the more familiar example of in-plane mounting, where s polarization corresponds to the TE case, and p polarization to TM. The switch is due to the altered groove orientation with respect to the field vectors.

B. Beamline Measurements

We tested an off-plane reflection grating for efficiency versus energy at two polarization orientations at the PTB soft X-ray beamline at the BESSY II electron storage ring [8, 9]. The PTB soft X-ray radiometry beamline utilizes an SX-700 plane grating

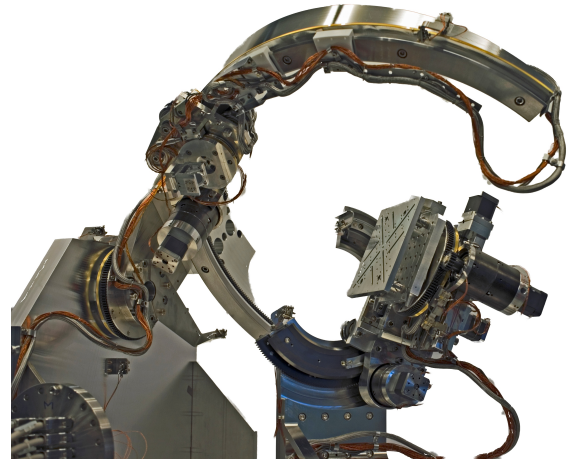


Fig. 2. Ellipso-scatterometer operated at the BESSY beamline designed to carry out scattering and reflectivity measurements at specified polarization orientation.

monochromator and covers a spectral range between 35–1700 eV. The new in vacuum ellipso-scatterometer of PTB, see Figure 2, is operated at this beamline and allows rotation about the axis of the incoming, linearly polarized (98.7%), photon beam. This facility therefore enables measurements at arbitrary polarization orientations. The SX700 beam is also extremely stable while tuning the energy: well below 0.001° in the azimuthal direction and negligible in the angle of incidence.

The grating tested at the PTB beamline has a laminar (rectangular) groove profile and an average groove spacing of 6033 grooves/mm on a 25 mm \times 32 mm \times 0.7 mm Si wafer coated with 80 nm of Au. The mounting orientation is illustrated in Figure 3. The grating was carefully aligned with a grazing incidence angle of 1.5° . Because the grating is not blazed and is thus not biased toward either side of zero order, it was mounted with the incident beam aligned parallel to the grating groove direction with no yaw (rotation about the grating normal axis) applied. The critical azimuthal alignment of the grooves with respect to the incident beam utilizes the symmetry of diffraction intensity and high order positions in the conical mount. The grating was first mounted with the electric field vector perpendicular to the plane of incidence (TM polarization) and measurements taken between 300 – 1500 eV in steps of 50 eV at 0° , $\pm 1^\circ$, $\pm 2^\circ$, $\pm 3^\circ$, and $\pm 4^\circ$ orders. The grating was then rotated 90° about the incident beam axis, and the same energy measurements were carried out in the TE configuration.

3. RESULTS AND MODELING

The efficiencies for 0^th through 4^th order TM and TE orientations measured at the PTB beamline are plotted in Figure 4. The measured TE efficiency is plotted using solid lines and TM using dashed lines. While statistical uncertainty in the reflectivity at each energy for single polarization is very small (near the plotted line width), we estimate that a small alignment error of $\sim 0.01^\circ$ in the azimuthal angle in our experiment between the two polarization orientations can completely account for the small differences observed between TM and TE efficiency. We therefore observe no significant polarization sensitivity.

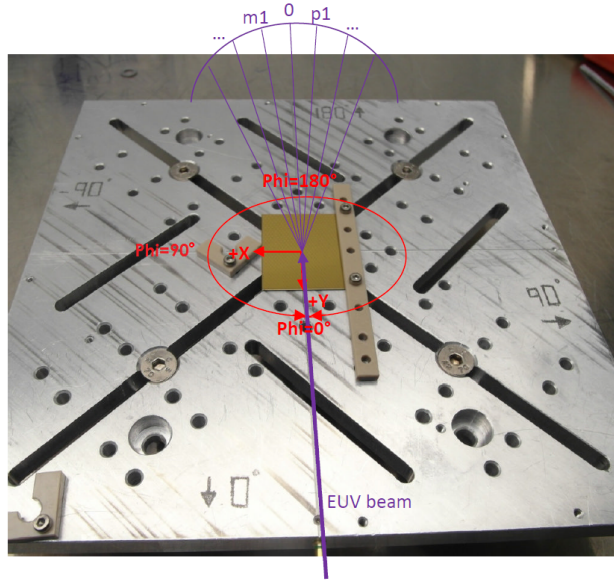


Fig. 3. Diagram of the grating mount orientation to the PTB beam. Light is incident from the bottom of the image at a graze angle of 1.5° with respect to the grating plane and parallel with the groove direction. The diffracted orders are observed along an arc at the detector plane, where positive orders are diffracted to the right of zeroth order in the image.

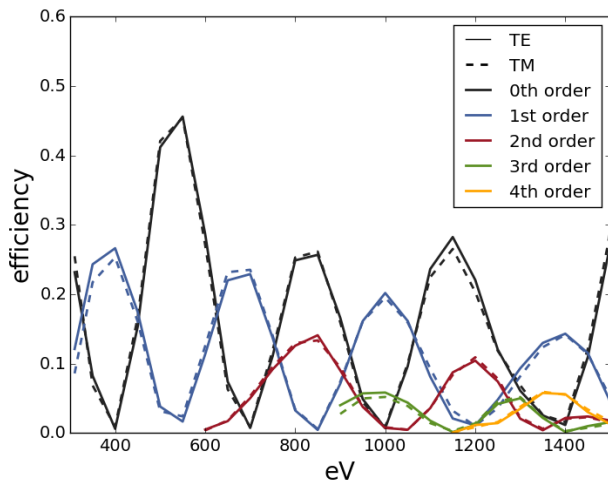


Fig. 4. Measured 0^{th} – 4^{th} order efficiencies of the laminar gratings measured at the PTB beamline. TE efficiencies are plotted as solid lines, while TM efficiencies are plotted as dashed lines. We observe no significant difference between the efficiencies for the two polarization orientations.

To compare our empirical results to theoretical predictions, efficiency calculations for the grating were carried out using PCGrate-SX v.6.1. PCGrate-SX is a software suite which models the efficiency of diffraction gratings using a boundary integral method for arbitrary groove profile and orientation, including in-plane and off-plane geometries. We model the laminar grating grooves as a sine trapezoidal profile, shown in Figure 5, which allows for realistic rounding of the groove corners apparent in

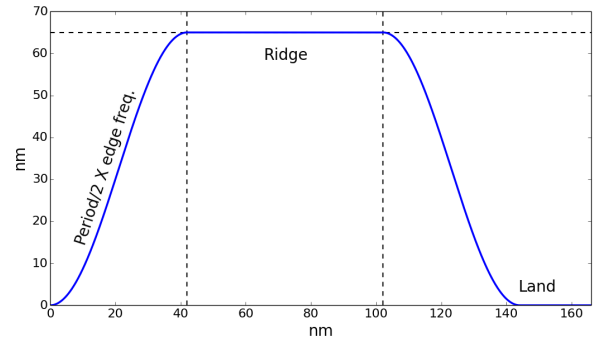


Fig. 5. Example of the sine trapezoidal groove profile used to model the laminar grating response with PCGrate-SX.

Scanning Electron Microscopy (SEM) measurements of the grating which were previously presented in McEntaffer et al. 2013 [2]. We investigated several probable groove profile responses by applying small variations to the model groove dimensions to best qualitatively describe the data within expectations.

PCGrate-SX v.6.1 was also used in the previous study which predicted significant polarization sensitivity for gratings in the off-plane mount [3]. It is important to note that the efficiency calculations in PCGrate-SX v.6.1 are made through application of the theory of invariance [10, 11] to express the off-plane efficiencies of a perfectly conducting grating in the form of a linear combination of efficiencies in the simplified in-plane geometry. However, the resulting efficiencies are limited to the idealized case of a grating with infinite conductivity. Goray & Schmidt 2010 [5] carried out more rigorous integral method calculations including finite conductivity for blazed, X-ray reflection gratings in the extreme off-plane mount, which demonstrate that the effect of real conductivity in this regime is non-negligible. The authors compare their results to those obtained under the assumption of perfect conductivity and find that the more rigorous treatment has little impact on the predicted TE efficiency. However, including finite conductivity strongly alters the predicted TM response. The resulting TM and TE efficiencies differ by no more than a few tenths of a percent. Thus, accounting for finite conductivity largely removes any polarization dependence on the predicted efficiency in the extreme off-plane mount at shallow graze angles.

Because there is not a predicted strong polarization effect for off-plane gratings when real surface conductivity is accounted for, the dominant polarization effect should in this case be due only to the reflection coefficients derived from Fresnel equations for a given surface material, incidence angle, and energy range. Thus, a small correction to produce TM efficiencies may be manually calculated from the TE predictions via these well known coefficients. For a grazing incidence angle, γ , the fraction of incident light that will be reflected, R , is given as (for derivation, see ch. 3 in [6])

$$R_{\text{TE}} = \left| \frac{n^2 \sin \gamma - \sqrt{n^2 - (1 - \cos^2 \gamma)}}{n^2 \sin \gamma + \sqrt{n^2 - (1 - \cos^2 \gamma)}} \right|^2 \quad (2)$$

$$R_{\text{TM}} = \left| \frac{\sin \gamma - \sqrt{n^2 - (1 - \cos^2 \gamma)}}{\sin \gamma + \sqrt{n^2 - (1 - \cos^2 \gamma)}} \right|^2, \quad (3)$$

for the TE and TM orientations, respectively. Here n is the

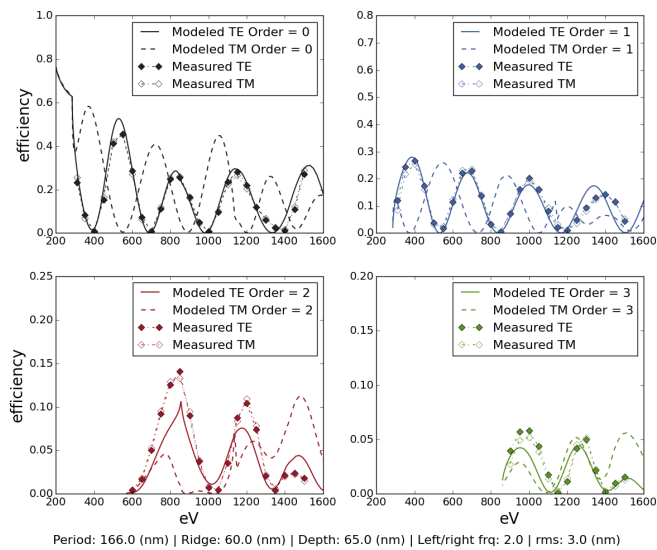


Fig. 6. Efficiency versus energy predicted by PCGrate-SX utilizing the invariance theorem (perfect conductivity). TE (TM) efficiency is plotted a solid (dashed) line. Each plot corresponds to a single order, with 0th order plotted top-left, 1st order top-right, 2nd order bottom-left, and 3rd order bottom-right. PTB measurements are plotted with filled (hollow) diamonds for the TE (TM) orientation. The sine trapezoidal profile parameters are listed at the bottom of the figure.

energy-dependent complex index of refraction of the grating surface material. As the graze angle, γ , becomes very shallow, the ratio of these coefficients approaches unity. At our energy range and shallow graze angle, the value of R_{TE}/R_{TM} differs from unity by only a few tenths of a percent.

We performed a correction of the perfect conductivity predicted TE efficiencies using the reflectivity coefficients to manually predict the expected TM response. We present the PCGrate-SX v.6.1 modeled efficiencies assuming perfect conductivity in Figure 6 and compare to the corrected efficiency predictions in Figure 7. In both plots, the measured TE and TM efficiencies are over-plotted as filled and hollow diamonds, respectively. We find that the perfect conductivity model predictions for the case of TE polarization gives good agreement to the measured response, but poor agreement for the case of TM polarization, supporting the calculations including finite conductivity presented by Goray & Schmidt 2010. After applying the reflectivity correction to predict TM response, the TE and TM predictions are now indistinguishable in Figure 7, consistent with our measurements. We note that the model rms roughness value that qualitatively best matches our empirical measurements is ~ 3 nm rms (shown in plot) while recent AFM measurements suggest a lower surface roughness value of 1.6 ± 0.5 nm rms.

We compared the corrected perfect conductivity results to two calculation methods that rigorously include finite surface conductivities. The first finite conductivity methods is PCGrate-SX v.6.6, an expanded version of the boundary integral equation solver that allows inclusion of finite conductivity for off-plane mounting. The finite conductivity integral method approach used by PCGrate-SX v.6.6 is detailed in Goray & Schmidt 2010, who find that it converges ~ 5 slower than the perfect conductivity model at the same level of accuracy in the case of

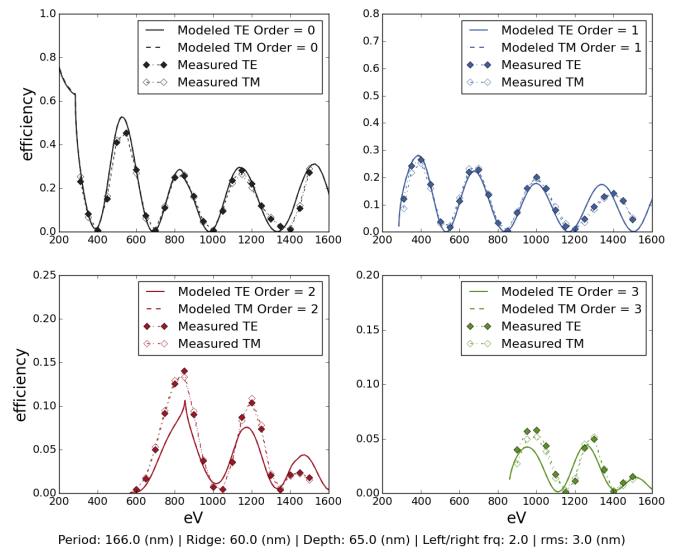


Fig. 7. PTB measurements over-plotted onto modeled efficiencies where the TM response has been manually calculated from the TE PCGrate-SX predictions corrected by reflectivity coefficients, in agreement with calculations assuming finite conductivity.

a Au-coated blazed off-plane grating. The second calculation method is JCMSuite, a rigorous Maxwell solver based on the finite-element method [12, 13]. A concern for Maxwell solvers in the x-ray regime is that the incident wavelength is several orders of magnitude smaller than the typical dimensions of the computational domain. This can be critical due to the increased computational effort. However, the dominant component of the wave vector is out-of-plane, enabling very fast and accurate solutions to the problem. Well-converged solutions were obtained for both the finite element Maxwell solver method JCMSuite and the boundary integral solver PCGrate-SX v.6.6.

All three models are plotted in Figure 8, showing good agreement between the finite conductivity boundary integral equation method, finite-element Maxwell solver, and the corrected perfect conductivity model. The three model results were calculated for the same idealized groove profile without surface roughness included. The finite-element Method of JCMSuite does not allow a direct modeling of surface roughness due to a discrepancy between the incident wavelength and the computational domain size. Correction to the calculated ideal grating diffraction efficiencies can be made using an approximation such as the well known Debye-Waller approach, or through a more rigorous Monte Carlo approach using measured real AFM profiles (see, e.g. Goray 2010 [14] and Ch. 12.9.10 in Antonakakis et al. 2014 [15]).

4. CONFIRMATION WITH BLAZED GRATING MEASUREMENTS

The diffraction efficiency of two holographically ruled 9° and 16° Pt-coated blazed gratings made by Jobin Yvon were previously measured at the PTB synchrotron facility in 2011. These gratings do not represent the current state-of-the-art in grating manufacturing, but can still be used to verify accurate modeling results. These measurements were taken with the gratings only in the TM orientation, largely due to mounting convenience and

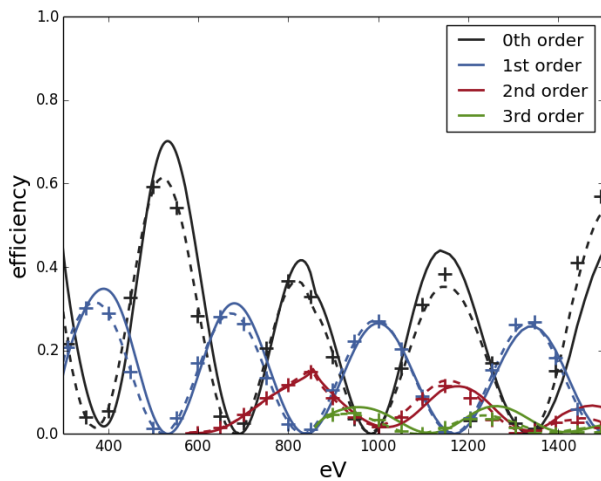


Fig. 8. Reflectivity coefficient corrected TM perfect conductivity efficiencies (solid lines), over-plotted with rigorous finite conductivity calculations using PCGrate V.6.6 (plus marks), and Maxwell solver calculations using JCMsuite (dashed lines).

lack of knowledge of the modeling inconsistencies. During the beamline tests, both gratings were mounted in their Littrow and anti-Littrow orientations. The Littrow orientation corresponds to an applied yaw to the grating such that the projection of the diffraction vector of the blazed wavelength on the xy plane is normal to the major grating facet, where the major facet is the grating face adjacent to the blaze angle. We define the anti-Littrow orientation as when the opposite yaw is applied to the grating.

New atomic force microscopy (AFM) measurements of the two blazed gratings were taken by the University of Pennsylvania which are shown in Figures 9 and 10. It is clear from the AFM results that the groove profiles of these gratings vary considerably over the grating surface. In order to account for profile variation, several groove profiles were extracted from the AFM data and used as direct input to PCGrate to estimate the predicted efficiency response. Nine profiles were extracted from grating U3787 (from measurements at two positions on the grating surface, and five from U3731 (for which we only obtained one measurement region at the grating center). For both gratings, PCGrate was run separately for each extracted AFM groove profile, yielding multiple values of modeled efficiency at each energy. The results of the individual profile models were used to make confidence intervals of one standard deviation about the average AFM model efficiency at each energy. We modeled both Littrow and anti-Littrow orientations using the AFM groove profile samples and compare to the experimental synchrotron measurements in Figures 11 and 12 for U3731 and U3787, respectively. The efficiency response is very sensitive to the groove profile, and the large variation in the actual groove profiles of the sample is apparent in the resulting AFM efficiency swaths. The measured synchrotron results for both gratings at multiple mounting geometries agree with the corrected TM orientation model predictions within the one standard deviation bounds derived from the sampled AFM groove profiles.

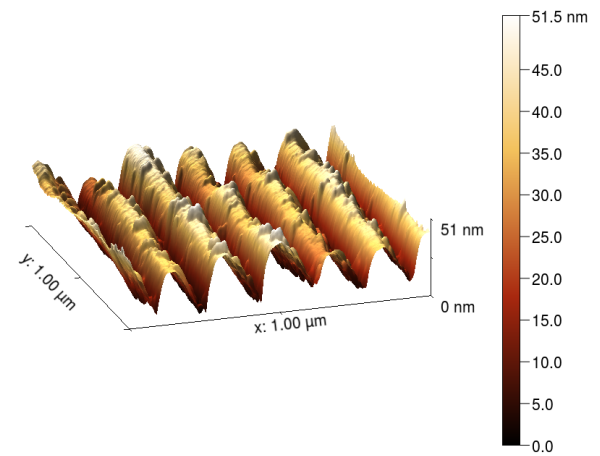


Fig. 9. AFM Measurements of 16° blazed, Pt-coated grating measured at the PTB beamline.

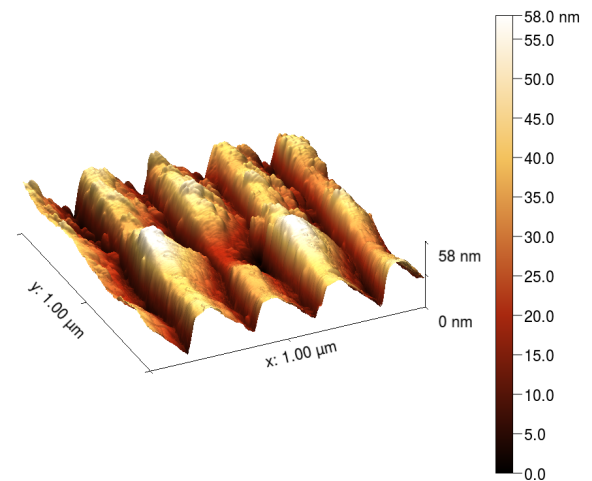


Fig. 10. AFM Measurements of 9° blazed, Pt-coated grating measured at the PTB beamline.

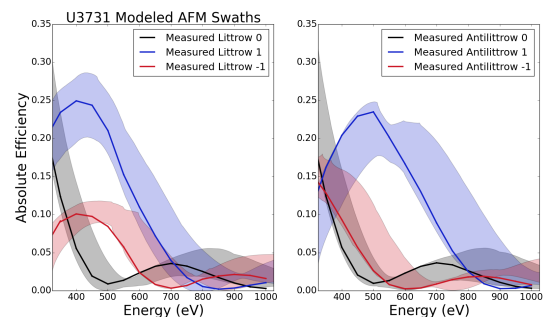


Fig. 11. Measured synchrotron response of the 16° blazed, Pt-coated grating measured at the PTB beamline (solid line) overplotted with the one standard deviation confidence interval of the model predicted response for a sample of groove profiles extracted from the AFM measurements.

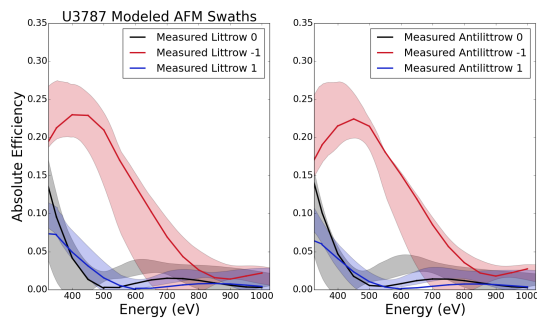


Fig. 12. Measured synchrotron response of the 9° blazed, Pt-coated grating measured at the PTB beamline (solid line) overlaid with the one standard deviation confidence interval of the model predicted response for a sample of groove profiles extracted from the AFM measurements.

5. DISCUSSION

We carried out experimental measurements of an off-plane grating with 6033 grooves/mm at a graze incidence of 1.5° and 0° yaw in the two fundamental linear polarization orientations and observe no polarization sensitivity. Our measurements support theoretical results by Goray & Schmidt 2010 [5] who demonstrate that the predicted strong polarization sensitivity of reflection gratings in the extreme off-plane mount disappears when real conductivity of the grating surface is taken into account. They show that calculations which make use of the invariance theorem, and thus assume perfect conductivity, strongly differ from the predicted response for finite conductivity gratings when light is incident in the TM orientation (E-field parallel to grating surface). However, the orthogonal TE orientation predictions are not strongly affected by the assumption of perfect conductivity, and so may still be used to predict grating response.

In agreement with the theoretical results of Goray & Schmidt 2010 [5], we find that we are able to produce accurate predictions for the TM polarization state by correcting the results of the perfect conductivity model TE efficiencies by the ratio of the reflectivity coefficients. Doing so yields predictions that match our empirical results for both linear polarization orientations for a laminar gratings and previous measurements of two blazed gratings at the TM orientation. Additionally, these corrected perfect conductivity results are in good agreement with calculations performed with finite surface conductivity via two methods: the expanded boundary integral method PCGrate-SX V.6.6, and the finite-element method JCMsuite. The more simple perfect conductivity model has an advantage of faster computation time, particularly in the case of a single rough grating layer, and therefore may be preferable to more rigorous methods for some applications in this regime.

6. FUNDING INFORMATION

NASA Earth and Space Science Fellowship (NNX13AM14H); NASA Strategic Astrophysics Technology grant (NNX15AC42G); NASA Astrophysics Research and Analysis (APRA) grant (NNX13AD03G). This work was also supported by the Russian Foundation for Basic Research (L.I.G.; grant 14-02-00391) and the Ministry of Education and Science of the Russian Federation (L.I.G.).

REFERENCES

1. R. L. McEntaffer, S. N. Osterman, W. C. Cash, J. Gilchrist, J. Flamand, B. Touzet, F. Bonnemason, and C. Brach, "X-ray performance of gratings in the extreme off-plane mount," in "Optics for EUV, X-Ray, and Gamma-Ray Astronomy," vol. 5168 of *Society of Photo-Optical Instrumentation Engineers (SPIE) Conference Series*, O. Citterio and S. L. O'Dell, eds. (2004), vol. 5168 of *Society of Photo-Optical Instrumentation Engineers (SPIE) Conference Series*, pp. 492–498.
2. R. McEntaffer, C. DeRoo, T. Schultz, B. Gantner, J. Tutt, A. Holland, S. O'Dell, J. Gaskin, J. Kolodziejczak, W. W. Zhang, K.-W. Chan, M. Biskach, R. McClelland, D. Iazikov, X. Wang, and L. Koecher, "First results from a next-generation off-plane X-ray diffraction grating," *Experimental Astronomy* **36**, 389–405 (2013).
3. L. I. Goray, "Rigorous efficiency calculations for blazed gratings working in in- and off-plane mountings in the 50–500 Å wavelengths range," in "Optics for EUV, X-Ray, and Gamma-Ray Astronomy," vol. 5168 of *Society of Photo-Optical Instrumentation Engineers (SPIE) Conference Series*, O. Citterio and S. L. O'Dell, eds. (2004), vol. 5168 of *Society of Photo-Optical Instrumentation Engineers (SPIE) Conference Series*, pp. 260–270.
4. J. F. Seely, L. I. Goray, B. Kjornrattanawanich, J. M. Laming, G. E. Holland, K. A. Flanagan, R. K. Heilmann, C.-H. Chang, M. L. Schattenburg, and A. P. Rasmussen, "Efficiency of a grazing-incidence off-plane grating in the soft-x-ray region," *Appl. Opt.* **45**, 1680–1687 (2006).
5. L. I. Goray and G. Schmidt, "Solving conical diffraction grating problems with integral equations," *Journal of the Optical Society of America A* **27**, 585 (2010).
6. D. Attwood, "Soft X-Rays and Extreme Ultraviolet Radiation," by David Attwood, ISBN 0521652146. Cambridge, UK: *Cambridge University Press*, pp. 486 August (1999).
7. H. Marlowe, R. L. McEntaffer, C. T. DeRoo, D. M. Miles, J. H. Tutt, C. Laubis, and V. Soltwisch, "Polarization sensitivity testing of off-plane reflection gratings," (2015).
8. F. Scholze, C. Laubis, C. Buchholz, A. Fischer, S. Plöger, F. Scholz, and G. Ulm, "Polarization dependence of multilayer reflectance in the EUV spectral range," in "Emerging Lithographic Technologies X," vol. 6151 of *Society of Photo-Optical Instrumentation Engineers (SPIE) Conference Series*, M. J. Lercel, ed. (2006), vol. 6151 of *Society of Photo-Optical Instrumentation Engineers (SPIE) Conference Series*, pp. 863–870.
9. C. Laubis, A. Kampe, C. Buchholz, A. Fischer, J. Puls, C. Stadelhoff, and F. Scholze, "Characterization of the polarization properties of PTB's EUV reflectometry system," in "Society of Photo-Optical Instrumentation Engineers (SPIE) Conference Series," vol. 7636 of *Society of Photo-Optical Instrumentation Engineers (SPIE) Conference Series* (2010), vol. 7636 of *Society of Photo-Optical Instrumentation Engineers (SPIE) Conference Series*, p. 2.
10. Petit, R. and Maystre, D., "Application des lois de l'électromagnétisme, à l'étude des réseaux," *Rev. Phys. Appl. (Paris)* **7**, 427–441 (1972).
11. D. Maystre and R. Petit, "Principe d'un spectromètre à réseau à transmission constante," *Optics Communications* **5**, 35–38 (1972).
12. J. Pomplun, S. Burger, L. Zschiedrich, and F. Schmidt, "Adaptive finite element method for simulation of optical nano structures," *physica status solidi (b)* **244**, 3419–3434 (2007).
13. V. Soltwisch, A. Haase, J. Wernecke, J. Probst, M. Schoengen, S. Burger, M. Krumrey, and F. Scholze, "Correlated Diffuse X-ray Scattering from Periodically Nano-Structured Surfaces," *ArXiv e-prints* (2015).
14. L. I. Goray, "Application of the rigorous method to x-ray and neutron beam scattering on rough surfaces," *Journal of Applied Physics* **108**, 033516 (2010).
15. T. Antonakakis, F. I. Baida, A. Belkhir, K. Cherednichenko, S. Cooper, R. Craster, G. Demésy, J. Desanto, G. Granet, B. Gralak, E. Popov, L. Goray, S. Guenneau, L. Li, D. Maystre, A. Nicolet, G. Schmidt, E. Skelton, B. Stout, F. Zolla, and B. Vial, *Gratings: Theory and Numeric Applications* (Popov, Institut Fresnel, 2014).